Enhancing the Sensitivity of Flexible Acoustic Wave Ultraviolet Photodetector with Graphene-Quantum-Dots Decorated ZnO Nanowires

Changshuai Yin[1], *Jianhui Wu*[1], *Jian Zhou*[1,*], *Dinghong Zhang*[1], *Zhijing Liu*[1], *Xudong Liu*[1], *Lizhu Liu*[1], Zhengjia Zhan[1], *Sean Garner*[2], *Yongqing Fu*[3]

[1]Engineering Research Center of Automotive Electrics and Control Technology, College of Mechanical and Vehicle Engineering, Hunan University, Changsha 410082, China

[2]Corning Research & Development Corporation, One River Front Plaza, Corning, NY 14831, USA

[3]Faculty of Engineering and Environment, Northumbria University, Newcastle upon Tyne, NE1 8ST, United Kingdom

*E-mail: jianzhou@hnu.edu.cn

Abstract: Graphene quantum dots decorated zinc oxide nanowires (GQDs@ZnO-NWs) were applied to enhance sensing performance of highly flexible and transparent surface acoustic wave (SAW) ultraviolet (UV) photodetectors made on ultra-thin flexible glass. The developed flexible SAW sensors possess better performance than that of the previously developed polymer based flexible SAW devices, due to insignificant acoustic loss of flexible glass substrate. UV sensitivity of the flexible glass based SAW sensors was enhanced by three times, and the response time was shorten by four times after the sensor was coated with the GQDs@ZnO-NWs hybrid nanomaterials. These improvements are mainly attributed to: (1) large specific surface areas of ZnO NWs which can generate a large number of

photon-generated carriers; (2) introduction of GQDs which can reduce the carrier recombination rate. The resonant frequency of flexible glass SAW UV photodetectors exhibited a good repeatability and stability in responses to cyclic changes of the UV lights at different wavelengths. They also maintained a good performance under a bending angle of ~30° for 200 times without apparent degradation, showing the excellent flexibility and stability of the UV photodetector.

Key words: Ultra-thin Glass; flexible SAW; GQDs@ZnO-NWs; UV sensing;

1. Introduction

Recently, flexible and wearable electronics become a cutting-edge research topic and have been explored for applications in human health monitoring, intelligent robot and man-machine interaction, as they are robust, small, comfortable to wear, and with low power consumption [1, 2]. Among them, flexible UV photo-detectors have been used in foldable displays, flexible mobile phones and wearable light sensors. They can be attached to the surface of the human skin to detect the intensity of the ultraviolet rays under the sun and protect the human body from skin diseases [3]. They can also be implanted into biological tissues and used to detect the internal structures of biological tissues [4]. At present, different types of flexible UV sensors have been developed, such as metal-semiconductor-metal UV detector [5], ohmic-contact UV detector [6], and Schottky barrier UV detector [7]. However, all these previously reported flexible UV sensors cannot be easily realized into wireless and passive sensing systems, and most of these flexible sensors are based on flexible organic substrates (such as polydimethylsiloxane-PDM, or polyethylene terephthalate-PET), which are not stable at high temperatures and limits the application of UV detectors in a harsh environment.

Surface acoustic wave (SAW) resonators are one of the essential Micro-Electro-Mechanical System (MEMS) resonators for sensing applications [8, 9], especially in wireless and passive sensing systems. When the surface of a piezoelectric material of SAW is coated with a layer of photoactive material or the piezoelectric material itself is photoactive in nature, the photo-generated carriers can effectively excite acoustic and electrical effects, thus can change the frequency, phase and amplitude of the SAW devices. This is sensing principle for ultraviolet (UV) light [10, 11]. However, the conventional SAW UV sensors are generally based on hard substrates such as $LiNbO_3$, Si, quartz, glass [12-15], thus they cannot be easily applied onto the curved and deformed surfaces, which limits their flexible electronics applications. To solve this problem, our research group has previously developed ZnO/polyimide (PI) based [16] and ZnO/Al foil based [17] flexible SAW UV sensors. However, polymer substrate generally has problems such as a large acoustic loss and low velocity, a low temperature tolerance and difficulty to be wafer level production. The amber color of PI limits its wide implementation in devices that require good transparency. Whereas the Al foil may produce metal ions which are contaminates during the MEMS manufacture processes. It also showsplastic deformation during bending which limits its applications for reliably flexible UV sensing. Therefore, it is still a great challenge to fabricate the flexible SAW UV sensors with good device performance, high flexibility and capability of wafer level production.

For high performance UV sensors, there is another challenge to develop new types of

UV active sensing material, which should have high electron mobility, good optical properties, and low cost. Compared with ZnO thin films, ZnO nanowires have larger specific surface area, which can generate a large number of photo-generated carriers [18]. Recently, to improve the sensitivity and response and recovery speed, ZnO nanostructures such as nanorods, nanowires, nanorings, nanohelix/nanorings, nanobelts, nanotubes, nanoflowers, nanowalls have been reported due their higher specific surface area and higher UV absorption efficiency [19, 20]. However, ZnO nanostructures have a higher refractive index. Therefore, when illuminated, a lot of photons will be emitted, thus reducing the photon absorption [21, 22]. In addition, due to the existence of large quantities of surface defects in ZnO nanostructures, many surface broken bonds and various surface defects will become luminescent centers of electron and hole recombination and non-radiant recombination [23].

To solve these problems, in this paper, we proposed a new type of hybrid nanomaterial of graphene quantum dots (GQDs) decorated ZnO nanowires (ZnO NWs) as the UV sensing layer on the ultra-thin glass based SAW UV sensor. It has several merits for this purpose:

(1) Ultra-thin glass is a suitable and inorganic substrate materials for flexible devices. It has a good optical quality and an optical transmission from 300 nm to 1500 nm showing negligible haze or absorption. In addition, it has recoverable bending characteristics and its surface quality is high with surface roughness generally smaller than 0.5 nm. Its thermal capability is good with a good stability up to ~600°C. Furthermore, environmental stability of ultra-thin glass is excellent in various conditions including high humidity and temperature, UV/sun light irradiation, and thermal cycling. Finally, the flexible glass can be wafer-level produced (up to 6-inch scale), suitable for fabricating flexible SAW UV sensors in a large

scale [24].

(2) Compared with ZnO thin films, ZnO nanowires have larger specific surface areas, which can generate a large number of photo-generated carriers [18]. In addition, the introduction of GQDs onto the surfaces of ZnO nanowires can reduce the carriers' recombination rate in the ZnO nanowires. GQDs, as a kind of cheap and non-toxic carbon nano-dots, have a high light-absorption rate in the UV region. The good energy band arrangement of GQDs can effectively improve the photosensitive characteristics of ZnO NWs [25]. These GQDs have a lower Fermi level and can be served as good electron acceptors for ZnO nanowires when they are under the UV irradiation, thus can capture the electrons in photon-generated carriers (as shown in Fig 1(a)). This will delay the potential recombination of holes and electrons of ZnO nanowires during UV irradiation, which is beneficial to improve the conductivity and UV sensing of the ZnO nanowires [26-29].

Without ultraviolet light, the oxygen molecules in the air will be adsorbed on the surface of ZnO NWs. These captured oxygen molecules will deprive free electrons of surface material and become oxygen ions to form a depletion region. The relevant chemical reactions are listed in the following two equations [30]:

$$O_2(g) + e^- \rightarrow O_2^-(\mathrm{ad}) \tag{4}$$

$$O_2(g) + 2e^- \rightarrow 2O^{2-}(\mathrm{ad}) \tag{5}$$

When the ZnO NWs are irradiated by UV light, the electrons on the valence band of ZnO will be transported from the valence band to the conduction band, leaving holes in the valence band and forming electron-hole pairs. The increase of carrier concentration will inevitably increase the conductivity of ZnO. However, the carriers will recombine with oxygen ions and release oxygen, this will decrease the conductivity. The specific reactions are shown in the following formula [30]:

$$O_2^-(\mathrm{ad}) + h^+ \rightarrow O_2(g) \tag{6}$$

$$2O^{2-} + 2h^+ \rightarrow O_2(g) \tag{7}$$

Here, the O_2 acts as the intermediate agent to enhance the carrier recombination. When the ZnO NWs are coated with GQDs, because the GQDs have lower Fermi levels, a large number of electrons will be adsorbed on the GQDs, thus the photo-generated carriers can be effectively separated, leaving a lot of holes in the ZnO NWs. Therefore, the introduction of GQDs can effectively separate the ZnO photogenerated carriers and reduce the carrier recombination rate, which significantly increase the photocurrent of GQDs@ZnO-NWs system than that of pure ZnO nanowires. Therefore, the conductivity of the ZnO is increased and the UV detection sensitivity is significantly improved.

Based on these assumptions, we have developed the flexible SAW sensors with excellent device performance and large UV sensor sensitivity. The flexible SAW devices exhibit a good repeatability and stability in responding to cyclic changes of the UV lights of various wavelengths and it maintains good performance under a bending angle of ~30° for 200 times without any apparent degradation, showing the excellent flexibility.

2. Experimental

Figure 1(b) shows a schematic diagram of a flexible SAW UV sensor enhanced with GQDs@ZnO-NWs nanocomposites based on flexible ultra-thin glass. ZnO films were deposited on flexible Corning® Willow® Glass (100 μm thickness) substrates using a direct-current (DC) magnetron sputtering system with a pure zinc target. The optimized deposition conditions were found to be [31]: substrate temperature of 100°C, chamber gas pressure of 2 Pa, O_2/Ar gas flow rates of 50/50, DC sputtering power of 200 W and bias voltage of −75 V. Standard UV photolithography and lift-off processes were applied to fabricate the interdigital transducers (IDTs, Cr/Au with thicknesses of 5/100 nm) of two-port SAW resonators, with different device wavelengths (λ) of 12, 16, 20 μm. The SAW devices had 50 pairs of IDTs with 100 reflectors and a metallization rate of 0.5. The aperture length was designed as 200 λ and the center distance between the two ports was 150 λ. Figure 2(c) shows a photo of the fabricated flexible SAW devices on a 3-inch flexible glass wafer. The fabricated SAW device was then diced into a die from the wafer and packaged onto a flexible printed circuit board (PCB) to demonstrate its flexibility as shown in Fig. 2(c).

ZnO NWs and GQDs were used as the UV enhanced sensing layer of flexible SAW device. Powders of ZnO nanowires (2 mg, obtained from XianFeng Company, China) were thoroughly diluted into deionized water to form 10 ml aqueous solution, which was then mixed with a 500 μl solution of GQDs (20 mg/ml, obtained from *ShiYiwei* Company, China) and magnetically stirred for one hour to obtain GQDs@ZnO-NWs mixed solution with a concentration of 1.2 mg/ml. The above solution was dripped onto the surface of the flexible SAW device, and dried on a hot plate at 80℃, thus forming a composite sensing layer for the SAW UV photodetector.

The cross-sectional structure and surface topography of the deposited ZnO film was characterized using a scanning electron microscope (SEM, ZEISS Sigma-300). Element composition and mapping analysis of mixed materials were performed using an energy dispersive spectroscopy (EDS) analyzer (Aztec X-MaxN 20 Oxford instruments). The stress value of the as-deposited film was calculated based on a biaxial strain model [32,33]. The film strain was calculated using: $\varepsilon = (c-c_0)/c_0$ along the c-axis, i.e., perpendicular to the substrate surface, where c and c_0 are the lattice parameters of the film and the strain-free lattice parameter of the bulk ZnO, respectively. The lattice parameter data were obtained from the X-ray diffraction (XRD, D5000, Siemens) peaks, using Cu-K_α radiation (λ = 1.5406 Å). The film stress values were calculated using the formula $\sigma = -233\times10^9\ (c-c_0)/c_0$ [32, 33]. The frequency responses of the fabricated SAW devices were measured using an Agilent N5247A network analyzer which accurately recorded the frequency, amplitude, insertion loss of the SAW devices. The effective electromechanical coupling coefficients, K^2, was calculated using $K^2 = \pi G_m(f_0)/4NB_s(f_0)$, where N is the finger pairs, $G_m(f_0)$ and $B_s(f_0)$ are the motional conductance and static susceptance of the input port at f_0, respectively [34]. For UV sensing tests, an ultraviolet lamp (ANUP 5252, Panasonic) was used to generate UV lights with different UV powers at a fixed wavelength of 365 nm. The UV lamp was positioned ~30 mm above the SAW sample. A Labview based program was developed to implement automated measurements and record the changes of frequency signals at different UV irradiation conditions as shown in Figure 1(d).

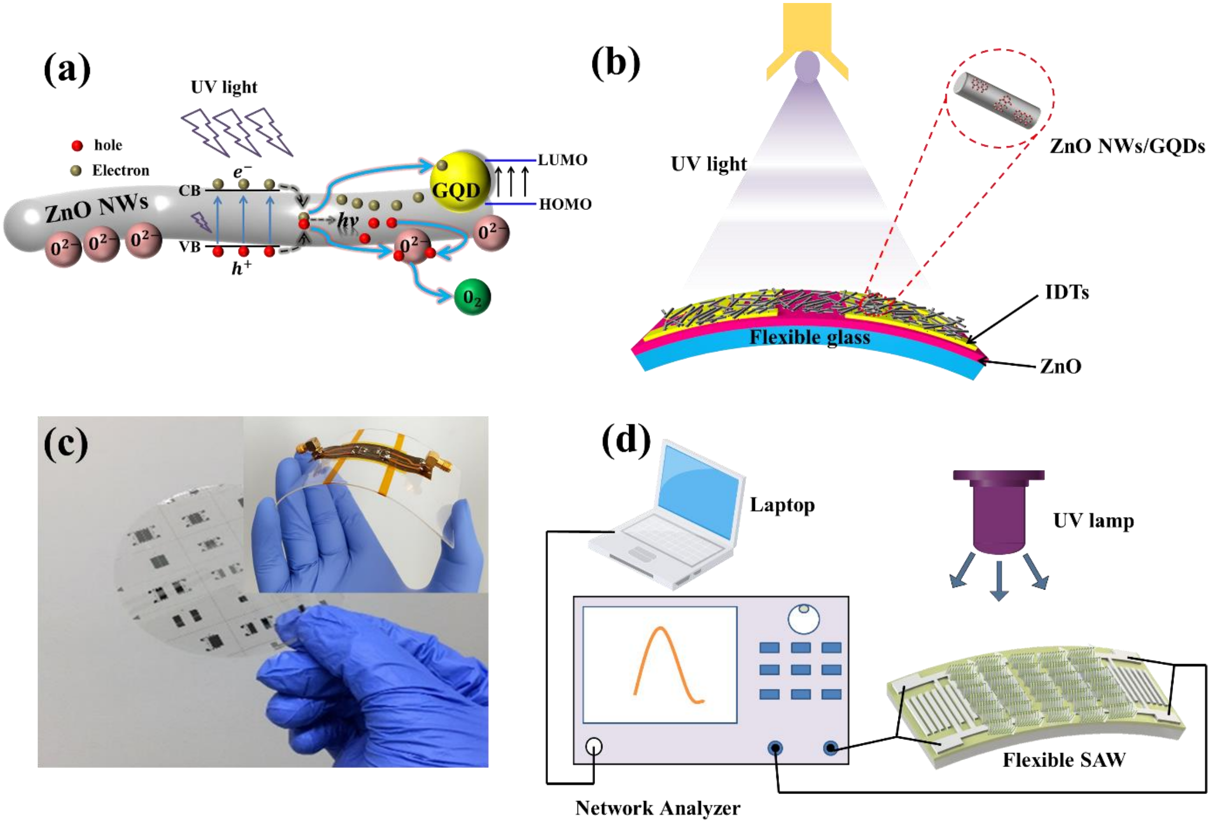

Figure 1: (a) Schematic diagram of UV mechanism of the GQDs@ZnO-NWs nano-composites under ultraviolet conditions; (b) the schematic diagram of a flexible SAW UV sensor using GQDs@ZnO-NWs composite nanomaterials; (c) flexible SAW devices on 3-inch flexible glass wafer and the fabricated SAW device can be diced into a die from a wafer and packaged onto the flexible PCB showing the flexibility. (d) Schematic diagram of UV test system

3. Results and Discussion

3.1 Material characterization and device performance

Figure 2(a) shows an SEM image of the cross-section of ZnO film (thickness of ~2.7 μm.) on ultra-thin glass, revealing columnar structures of the ZnO nanocrystals perpendicular to the ultra-thin glass substrate. The stress value of the ZnO film deposited on the flexible glass is about 110 MPa, which is lower than previous work [35]. Results show that the ZnO film on the flexible substrate have high crystal quality with desired crystal orientation, low stress and large columnar structures which are beneficial to the SAW device performance. Figure 2(b) shows the EDS mapping of GQD@ZnO-NWs composite materials, proving that the GQDs are indeed coated on the ZnO nanowires. Figure 2(c) shows an optical image of the flexible SAW on ultra-thin glass with the wavelength of 20 μm, showing that the IDTs are uniform with good quality on ZnO/ultra-thin glass substrate.

Figures 2(d-f) shows the transmission (S_{21}) spectra of the flexible SAW devices with the composite layer of GQDs@ZnO-NWs and wavelengths of 12 μm, 16 μm, and 20 μm. All the flexible SAW devices showed obvious Rayleigh wave resonance peaks, which have the transmission signal amplitude between ~40 to 45 dB. This transmission signal is ~160% higher than that the previous polymer based flexible SAW devices [36], demonstrating the good device performance of flexible glass based SAW device due to the relatively low acoustic loss of flexible glass and the highly (0002) orientated of ZnO films. The resonant frequencies are 220.18 MHz, 169.60 MHz and 138.25 MHz for the SAW wavelengths of 12 μm, 16 μm and 20 μm, respectively, corresponding the calculated phase velocity to be 2642 m/s, 2711 m/s, and 2763 m/s. When the wavelength is increased, more energy are dispersed into the glass substrate, leading to a higher phase velocity of the layered structure, which is consistent with the observation from other layered structure SAW devices [37]. The K^2 values were found to be ~2.58% , ~2.89%, and ~2.52%, for the wavelength of 12 μm, 16 μm and 20 μm, respectively, which are much higher than that of previous polymer based flexible SAW devices [34]. The main reason is that the sound loss of SAW devices based on ultra-thin glass substrates is smaller than that of polymers.

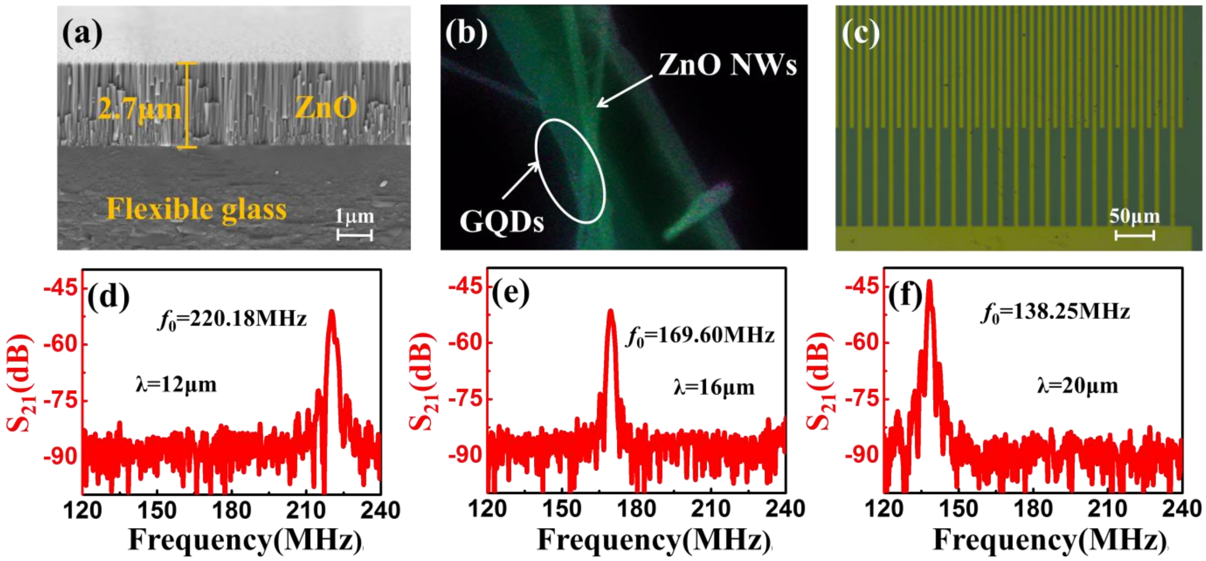

Figure 2: (a) The SEM image of ZnO/flexible glass; (b) The EDS mapping of GQDs@ZnO-NWs; (c) the optical image of the flexible SAW on flexible glass; (d~f) Characterization of transmission (S_{21}) parameters of the device after spin-coating GQDs@ZnO-NWs solution with wavelength of 12 μm, 16 μm; and 20 μm

3.2 UV sensing for flexible SAW sensor without GQDs@ZnO-NWs sensitive layer

The changes of the resonant frequency the flexible ZnO/glass SAW device without the composite sensing layer under different UV intensities have been investigated and the results are shown in Figures 3(a-c). Results showed that the flexible glass based SAW sensor is sensitive to UV light, and the frequency shifts (Δf) of the flexible SAW increases with the increase in UV light intensity for the devices at different SAW wavelengths. The UV light responses of the flexible glass based SAW sensors are mainly attributed to the photo-generated free carriers that change the conductivity of the ZnO film surface layer of the SAW device. When the UV light is exposed to the ZnO, electrons in the valence band move into the conduction band, leading to the generation of free electron–hole pairs which are confined to the surface layer of the ZnO film. The free carriers on the surface of SAW device will interact with the surface acoustic field, resulting in a change in the transmission characteristics. The change in the conductivity leads to the change in the resonant frequency of the SAW sensor, which is given by the following formula [38]:

$$\frac{\Delta f}{f_0} = \frac{\Delta v}{v_0} = -\frac{K^2}{2}\frac{(\sigma d)^2}{(\sigma d)^2+(v_0 C_s)^2} \tag{1}$$

where f_0, v_0 are the initial resonance frequency and the propagation velocity on the surface of piezo film; $\Delta f, \Delta v$ are the frequency shift and velocity change of SAW; K^2 is the electromechanical coupling coefficient; $C_s = \varepsilon_0(1+\varepsilon_r)$, ε_0 is the vacuum dielectric constant, ε_r is the relative dielectric constant of the piezoelectric substrate material; σ is the conductivity of the piezoelectric film, and d is the thickness of the piezoelectric film.

The SAW devices with different wavelengths or different frequencies show quite different UV responses. For the same UV intensity of 180 mW/cm^2, the frequency shifts are ~36 kHz, ~22 kHz, and ~12 kHz for the SAW wavelengths of 12 μm, 16 μm, and 20 μm respectively, indicating that a shorter wavelength (based on $f = v/\lambda$; this is meaning higher resonance frequency) leads to a higher UV sensitivity. The main reason for this is that the shorter the wavelength, the more energy is concentrated near the device's surface, which causes an increase in speed and increased changes in frequency.

The repeatability and stability of the flexible SAW UV light sensors have been investigated. Figure 3(d) shows the cyclic responses of the various resonant frequencies of the SAW sensor when it was illuminated cyclically with a light intensity of 170 mw/cm^2. Figure 3(e) shows the repeatability test of a device with a wavelength of 20 μm under different UV intensities. The resonant frequencies are decreased rapidly when the UV light is switched on, and become saturated after a transient time. Figure 3(f) shows that frequency responses to the light intensity are changed from 50 mw/cm^2 to 110 mW/cm^2, showing an excellent UV intensity sensitivity without phenomenon of frequency disturbance. These results clearly show that when the ultraviolet light intensity changes, the developed SAW sensor has good repeatability, stability and light intensity sensitivity.

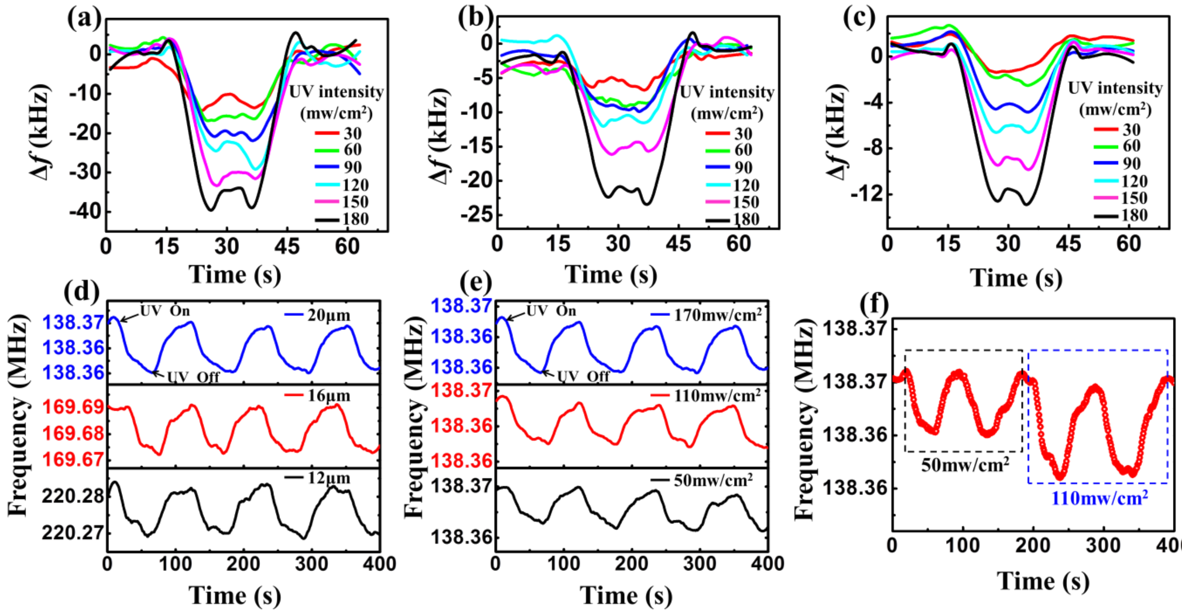

Figure 3: The resonance frequency of the flexible SAW sensor without GQDs@ZnO-NWs is shifted by Δf under the irradiation of ultraviolet light of different light intensity;(a)12 μm; (b)16 μm; (c) 20 μm; (d) Repeatability test for devices with wavelengths of 12μm, 16μm, and 20μm under 170mw/cm^2 light;(e) Repeatability test of a device with a wavelength of 20μm under the conditions of light intensity of 50mw/cm^2, 110mw/cm^2, and 170mw/cm^2;(f) The light intensity adaptability of flexible SAW device

3.3 UV sensing for flexible SAW with GQDs@ZnO-NWs sensitive layer

Figures 4(a-c) show the changes of the resonant frequency for the flexible glass based SAW device with a composite sensing layer of GQDs@ZnO-NWs under different UV intensities. Similar to those without nano-sensing layer, the frequency shifts of the flexible SAW with the sensing layer increase significantly with the UV light intensity, and the higher resonance frequency (shorter wavelength) leads to a larger frequency shift. In addition, the frequency shifts of the flexible SAW device with the GQDs@ZnO-NWs sensitive layer have much larger frequency shifts for all the different tested cases. For example, the maximum frequency shifts at a UV intensity of 180 mw/cm^2 for the SAW device with the nanostructured layer are ~57 kHz, ~46 kHz, and ~39 kHz with the wavelengths of 12 μm, 16 μm, and 20 μm respectively. These values are much larger than those without adding composite sensing layer.

Figures 4(d-f) compare frequency shifts of the flexible SAW device with/without a GQDs@ZnO-NWs sensitive layer for different wavelengths at a UV intensity of 50 mw/cm^2, tested for 5 cycles. Results showed that all the flexible SAW devices show good repeatability and stability. After coated with composite sensing layer, the resonance frequency shifts of the devices are changed from ~9 kHz, ~7 kHz, and ~5 kHz for wavelengths of 12 μm, 16 μm, and 20 μm respectively, to values of ~ 28 kHz, ~23 kHz, ~15 kHz, respectively, about three times higher than that of SAW without sensitive layer.

The UV light sensitivity of the SAW devices is defined as [39]:

$$S = \frac{1}{f_0}\frac{\Delta f_{UV}}{I_{\Delta UV}} \qquad (2)$$

where S is the sensitivity of the sensor; f_0 is the resonant frequency of the sensor; Δf_{UV} is the frequency offset caused by ultraviolet light; $I_{\Delta UV}$ is the change in light intensity. Figure 4(g) illustrates that there is a linear relationship between the frequency shift (Δf) and the light intensity of the device with/without GQDs@ZnO-NWs sensing layers for flexible SAW devices. The calculation results are listed in Table 1. Results showed that the flexible glass based SAW devices with a GQDs@ZnO-NWs sensitive layer have a good linearity and a larger UV sensitivity compared with those without GQDs@ZnO-NWs sensitive layer.

Table 1: Resonant frequency, UV sensitivity of different flexible SAW

Wavelength & without/with sensitive layers	Resonant frequency (MHz)	Sensitivity(mw/cm^2)$^{-1}$

12um ×	220.28	0.92ppm
16um ×	169.69	0.71ppm
20um ×	138.37	0.48ppm
12um √	220.20	1.53ppm
16um √	169.44	1.66ppm
20um √	138.25	1.48ppm

Explanation: ×:without GQDs@ZnO-NWs sensitive layer ; √ with GQDs@ZnO-NWs sensitive layer

Figures 4(h) and 4(i) show the response time and recovery time of the flexible SAW with/without the GQDs@ZnO-NWs sensing layer, and the response time has been improved by about 3~4 times after applying the nanolayer. The main reason is that the introduction of GQDs@ZnO-NWs composite materials will accelerate the process of adsorption and desorption of oxygen molecules on the surface of the device, which will shorten the response time and recovery time [40].

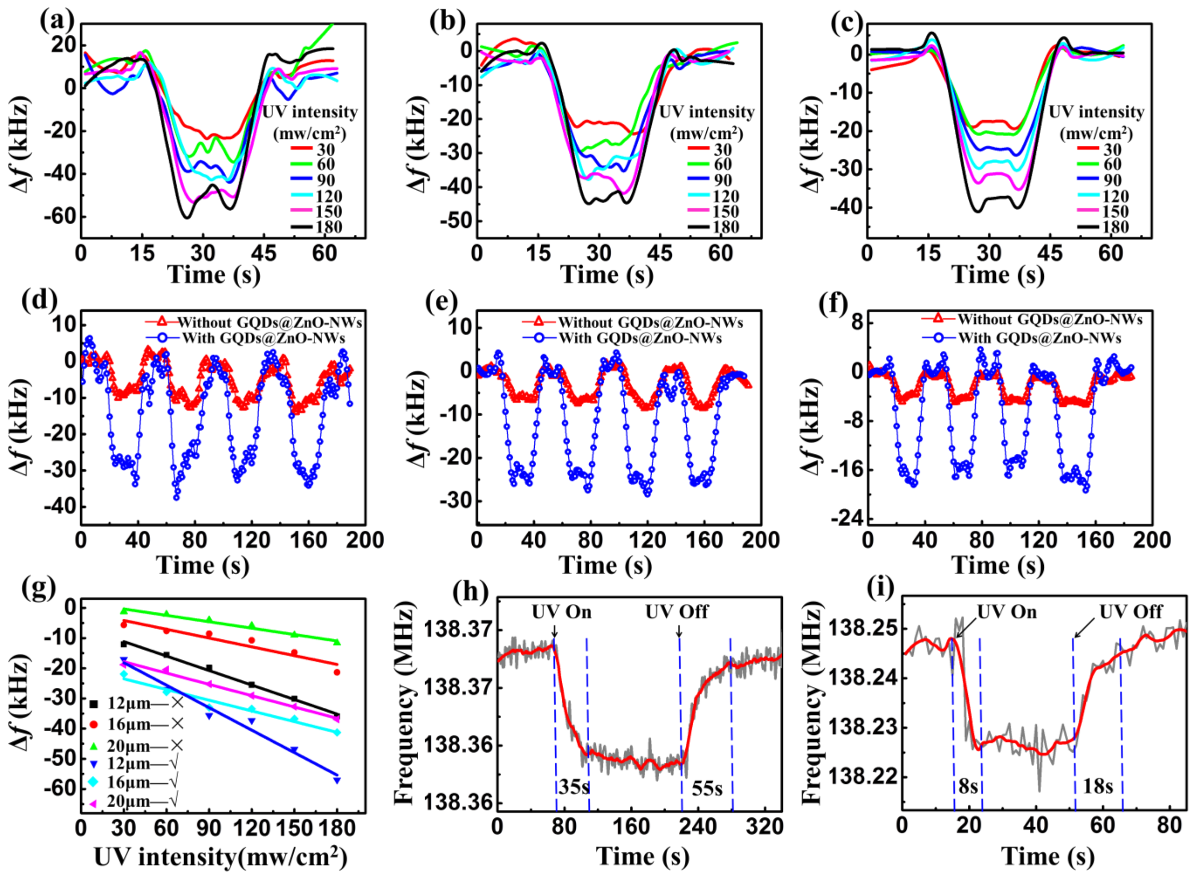

Figure 4: The resonance frequency of the flexible SAW sensor with GQDs@ZnO-NWs is shifted by Δf under the irradiation of ultraviolet light of different light intensity; (a)12μm;

(b)16μm; (c)20μm; Repeatability test of different devices with/without GQDs@ZnO-NWs sensitive layer at a light intensity of 50mw/cm^2; (d)12μm; (e)16μm; (f)20μm; (g) The relationship between frequency offset and light intensity of each device with/without GQDs@ZnO-NWs sensitive layer (note: '×'means without GQDs@ZnO-NWs sensitive layer; '√'means with GQDs@ZnO-NWs sensitive layer); (h) Device response time and recovery time when UV light is turned on and off without GQDs@ZnO-NWs sensitive layer;(i) Device response time and recovery time when UV light is turned on and off with GQDs@ZnO-NWs sensitive layer

3.4. Temperature sensitivity and Flexible bending characteristics

The flexible SAW devices are generally sensitive to temperature changes. Figure 5(a) shows the resonant frequencies of the flexible glass based SAW devices, measured as a function of temperature. The frequencies decrease linearly with the increase of temperature. The temperature coefficients of frequency (TCF) values for the fabricated temperature sensors, defined as $\Delta f/\Delta T f_0$, are 30.2, 20.9 and 21.9 ppm/K, for the wavelengths of 12 μm, 16 μm and 20 μm, respectively. These were comparable with those of the conventional rigid glass based ZnO film SAW devices [41].

Figure 5(b) shows the changes of resonant frequency for the sensor at various temperatures for the wavelength of 16 μm. When the ambient temperature was increased from 40℃ to 60℃ and then decreased back to 40℃, the resonance frequency was increased by ~80 kHz and then decreased by ~ 80 kHz, respectively. Whereas the resonance frequency was shifted ~160 kHz, as the temperature was changed from 20℃ to 80℃. This is consistent with those shown in Fig. 5(c), in which the frequency is shifted by ~40 kHz for a temperature change of 10℃。

The performance of flexible SAW devices upon bending was further investigated. The flexible SAW sensor was wire bonded onto the flexible circuit board, and then attached to a thin steel sheet with a thickness of 0.1 mm, as shown in Figure 5(c). Bending measurement of the ZnO/glass sensor was carried out using a tensile tester (Shimadzu, model AGS-X, 100 N, China) at room temperature, with a constant velocity of 40 mm/min and a clamp distance of 2 cm. Figure 5(d) show the changes of the transmission spectra before and after bending for 10, 30, 80, 100, 150, and 200 times at the bending angle of ~30°. It is clear that the device maintains a good performance under a bending angle of ~30° for 200 times and shows no apparent degradation in performance. This experiment demonstrated the excellent flexibility of the flexible SAW devices based on flexible glass.

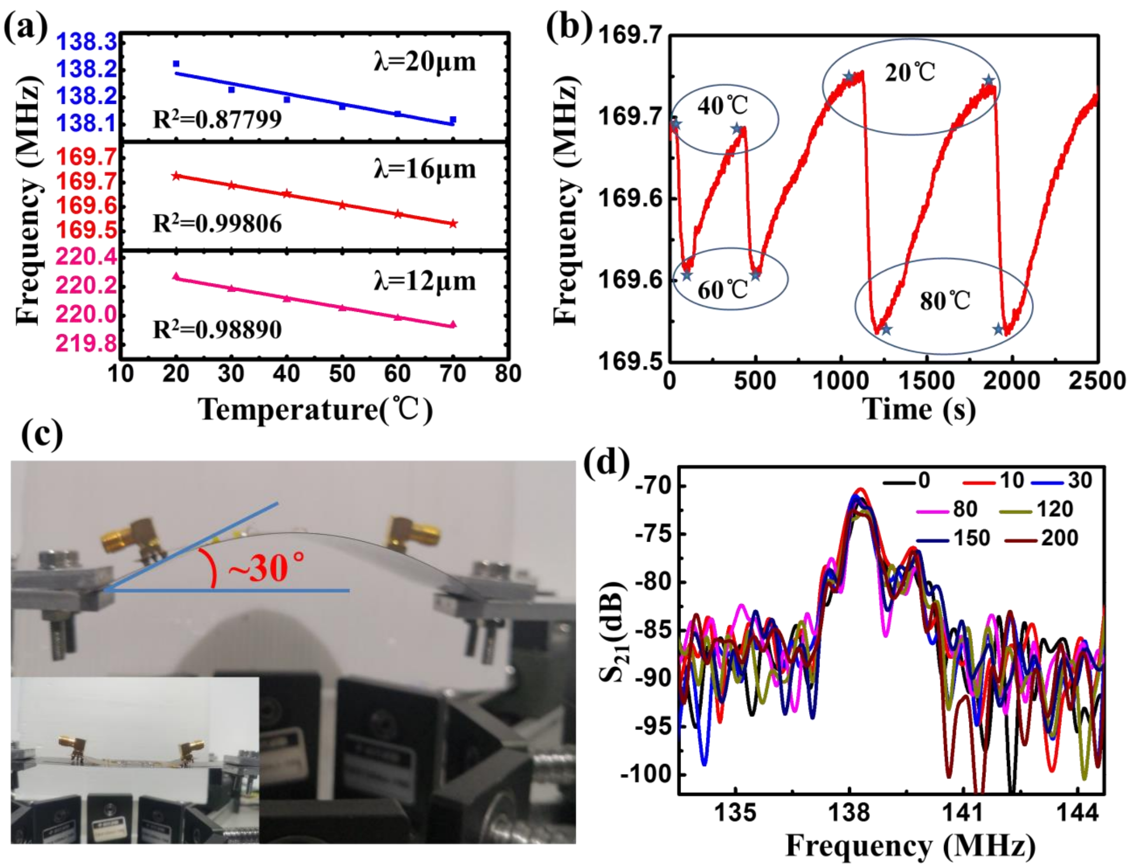

Figure 5: (a) The relationship between resonance frequency and temperature of the different wavelength SAW devices;(b) Variation of the resonant frequency of the device at different temperatures;(c) The display of the maximum bending state of the flexible SAW;(d) Changes in the S_{21} parameters of the device after 10, 30, 80, 120, 150, 200 cyclic bending tests

4. Conclusion

This paper reported an ultra-thin glass based highly flexible and transparent SAW UV sensors based on GQDs@ZnO-NWs nano-hybrid materials. The flexible SAW sensors has high effective electromechanical coupling coefficients of and large signal amplitude (40 dB), which is ~160% higher than that the previous polymer based flexible SAW devices, demonstrating the good device performance of flexible glass based SAW device due to insignificant acoustic loss of flexible glass. The UV sensitivity of flexible SAW with GQDs@ZnO-NWs hybrid nanomaterials is increased by 3 times, and the response time is shorten by 4 times due to the large specific surface area of ZnO nanowires. These can generate a large number of photo-generated carriers and the GQDs can reduce the carrier recombination rate. The shifts of resonant frequency of flexible SAW devices exhibit a good repeatability and stability in responses to the cyclic change of the UV light for various wavelengths and it maintains good performance under a bending angle of ~30° for 200 times without visible degradation, showing the excellent flexibility. The frequencies are decreased linearly with the increase of temperature with a good linear correlation.

Acknowledgments

This work was supported by the General Program of National Natural Science Foundation of China (No.52075162), the Key Research Project of Hunan Province (2019GK2111), Innovation Leading Program of New and High-tech Industry of Hunan Province (2020GK2015), the Key Research Project of Guangdong Province

(2020B0101040002) and the Natural Science Foundation of Changsha, the UK Engineering and Physical Sciences Research Council (EPSRC) grants EP/P018998/1.

References

[1] D. Vilela, A. Romeo, S. Sanchez, Flexible sensors for biomedical technology, Lab Chip, 16(2016) 402-8.
[2] K. Takei, W. Honda, S. Harada, et al., Toward flexible and wearable human-interactive health-monitoring devices, Adv Healthc Mater, 4(2015) 487-500.
[3] M.E. Lee, A.M. Armani, Flexible UV Exposure Sensor Based on UV Responsive Polymer, ACS Sens., 1(2016) 1251-5.
[4] G. Shin, A.M. Gomez, R. Al-Hasani, et al., Flexible Near-Field Wireless Optoelectronics as Subdermal Implants for Broad Applications in Optogenetics, Neuron, 93(2017) 509-21 e3.
[5] H.T. Zhou, L. Li, H.Y. Chen, et al., Realization of a fast-response flexible ultraviolet photodetector employing a metal–semiconductor–metal structure InGaZnO photodiode, RSC Adv., 5(2015) 87993-7.
[6] W. Tian, C. Zhang, T. Zhai, et al., Flexible ultraviolet photodetectors with broad photoresponse based on branched ZnS-ZnO heterostructure nanofilms, Adv. Mater., 26(2014) 3088-93.
[7] S. Lu, J. Qi, S. Liu, et al., Piezotronic interface engineering on ZnO/Au-based Schottky junction for enhanced photoresponse of a flexible self-powered UV detector, ACS Appl Mater Interfaces, 6(2014) 14116-22.
[8] J. Zheng, J. Zhou, P. Zeng, et al., 30 GHz surface acoustic wave transducers with extremely high mass sensitivity, Appl. Phys. Lett., 116(2020).
[9] Z. Chen, J. Zhou, H. Tang, et al., Ultrahigh-Frequency Surface Acoustic Wave Sensors with Giant Mass-Loading Effects on Electrodes, ACS Sens, (2020).
[10] Y.Q. Fu, J.K. Luo, N.T. Nguyen, et al., Advances in piezoelectric thin films for acoustic biosensors, acoustofluidics and lab-on-chip applications, Prog. Mater Sci., 89(2017) 31-91.
[11] V. Chivukula, D. Ciplys, M. Shur, et al., ZnO nanoparticle surface acoustic wave UV sensor, Appl. Phys. Lett., 96(2010).
[12] W. Li, Y.J. Guo, Q.B. Tang, et al., Highly sensitive ultraviolet sensor based on ZnO nanorod film deposited on ST-cut quartz surface acoustic wave devices, Surf. Coat. Technol., 363(2019) 419-25.
[13] P. Sharma, K. Sreenivas, Highly sensitive ultraviolet detector based on ZnO/LiNbO3 hybrid surface acoustic wave filter, Appl. Phys. Lett., 83(2003) 3617-9.
[14] W. Wang, H. Gu, X. He, et al., Thermal annealing effect on ZnO surface acoustic wave-based ultraviolet light sensors on glass substrates, Appl. Phys. Lett., 104(2014).
[15] C.-L. Wei, Y.-C. Chen, C.-C. Cheng, et al., Highly sensitive ultraviolet detector using a ZnO/Si layered SAW oscillator, Thin Solid Films, 518(2010) 3059-62.
[16] X.L. He, J. Zhou, W.B. Wang, et al., High performance dual-wave mode flexible surface acoustic wave resonators for UV light sensing, J. Micromech. Microeng., 24(2014).
[17] X. Tao, H. Jin, M. Mintken, et al., Three-Dimensional Tetrapodal ZnO Microstructured Network Based Flexible Surface Acoustic Wave Device for Ultraviolet and Respiration Monitoring Applications, ACS Appl. Nano Mater., 3(2020) 1468-78.
[18] C. Soci, A. Zhang, X.Y. Bao, et al., Nanowire photodetectors, J Nanosci Nanotechnol, 10(2010) 1430-49.
[19] L. Sang, M. Liao, M. Sumiya, A comprehensive review of semiconductor ultraviolet photodetectors: from thin film to one-dimensional nanostructures, Sensors (Basel), 13(2013) 10482-518.

[20] Y.J. Guo, C. Zhao, X.S. Zhou, et al., Ultraviolet sensing based on nanostructured ZnO/Si surface acoustic wave devices, Smart Mater. Struct., 24(2015).
[21] M. Caglar, S. Ilican, Y. Caglar, et al., Electrical conductivity and optical properties of ZnO nanostructured thin film, Appl. Surf. Sci., 255(2009) 4491-6.
[22] T.N. Lin, S.R.M. Santiago, C.T. Yuan, et al., Enhanced Performance of GaN-based Ultraviolet Light Emitting Diodes by Photon Recycling Using Graphene Quantum Dots, Sci. Rep., 7(2017) 7108.
[23] J.E. Piprek, Nitride semiconductor devices: principles and simulation, New Jersey: John Wiley& Sons, (2007) 24.
[24] S. Garner, S. Glaesemann, X. Li, Ultra-slim flexible glass for roll-to-roll electronic device fabrication, Appl. Phys. A, 116(2014) 403-7.
[25] S. Dhar, T. Majumder, S.P. Mondal, Graphene Quantum Dot-Sensitized ZnO Nanorod/Polymer Schottky Junction UV Detector with Superior External Quantum Efficiency, Detectivity, and Responsivity, ACS Appl. Mater. Interfaces, 8(2016) 31822-31.
[26] Y. Li, Y. Hu, Y. Zhao, et al., An electrochemical avenue to green-luminescent graphene quantum dots as potential electron-acceptors for photovoltaics, Adv. Mater., 23(2011) 776-80.
[27] W. Han, J. Kim, H.H. Park, Control of electrical conductivity of highly stacked zinc oxide nanocrystals by ultraviolet treatment, Sci. Rep., 9(2019) 6244.
[28] M. Ebrahimi, M. Samadi, S. Yousefzadeh, et al., Improved Solar-Driven Photocatalytic Activity of Hybrid Graphene Quantum Dots/ZnO Nanowires: A Direct Z-Scheme Mechanism, ACS Sustainable Chem. Eng., 5(2016) 367-75.
[29] Z. Wang, X. Zhan, Y. Wang, et al., A flexible UV nanosensor based on reduced graphene oxide decorated ZnO nanostructures, Nanoscale, 4(2012) 2678-84.
[30] Y. Zhang, Y. Cai, J. Zhou, et al., Surface acoustic wave-based ultraviolet photodetectors: a review, Science Bulletin, 65(2020) 587-600.
[31] J. Zhou, J. Zheng, X. Shi, et al., Graphene-Based Fully Transparent Thin Film Surface Acoustic Wave Devices for Sensing and Lab-on-Chip Applications, J. Electrochem. Soc., 166(2019) B432-B40.
[32] J. Zhou, X. Tao, J. Luo, et al., Nebulization using ZnO/Si surface acoustic wave devices with focused interdigitated transducers, Surf. Coat. Technol., 367(2019) 127-34.
[33] A. Khorsand Zak, W.H. Abd. Majid, M.E. Abrishami, et al., X-ray analysis of ZnO nanoparticles by Williamson–Hall and size–strain plot methods, Solid State Sci., 13(2011) 251-6.
[34] C. Campbell, Surface Acoustic Wave Devices for Mobile and Wireless Communications, Four-Volume Set: Academic press; 1998.
[35] M. Mekhnache, A. Drici, L. Saad Hamideche, et al., Properties of ZnO thin films deposited on (glass, ITO and ZnO:Al) substrates, Superlattices Microstruct., 49(2011) 510-8.
[36] X.L. He, D.J. Li, J. Zhou, et al., High sensitivity humidity sensors using flexible surface acoustic wave devices made on nanocrystalline ZnO/polyimide substrates, J. Mater. Chem. C, 1(2013).
[37] Y. Nakagawa, Elastic ‐ surface ‐ wave temperature coefficients of delay line with ZnO thin film, Appl. Phys. Lett., 31(1977) 56-7.
[38] A. Ricco, S. Martin, T.J.S. Zipperian, et al., Surface acoustic wave gas sensor based on film conductivity changes, 8(1985) 319-33.
[39] H.-F. Pang, Y.-Q. Fu, Z.-J. Li, et al., Love mode surface acoustic wave ultraviolet sensor using ZnO films deposited on 36° Y-cut LiTaO3, Sens. Actuators, A, 193(2013) 87-94.
[40] C. Fu, K.J. Lee, K. Lee, et al., Low-intensity ultraviolet detection using a surface acoustic-wave sensor with a Ag-doped ZnO nanoparticle film, Smart Mater. Struct., 24(2015).

[41] X.-G. Tian, H. Liu, L.-Q. Tao, et al., High-resolution, high-linearity temperature sensor using surface acoustic wave device based on LiNbO3/SiO2/Si substrate, AIP Adv., 6(2016).